Melting and freezing of embedded nanoclusters

Frédéric Caupin*
Laboratoire de Physique Statistique de l'Ecole Normale Supérieure, associé au CNRS et aux Universités Paris 6 et Paris 7, 24 rue Lhomond 75005 Paris, France

(Received 21 February 2008; revised manuscript received 6 April 2008; published 12 May 2008)

Small crystals are known to melt at a different temperature than the bulk; it is usually lower for freestanding nanocrystals. However, the size-dependent melting temperature is often analyzed with approximate formulas, corresponding to the limits of metastability of the solid cluster, instead of accounting for nucleation at an intermediate temperature. In addition, the advent of nanofabrication of inclusions in a host matrix adds a parameter to the problem: the different interactions of the matrix with the solid and the liquid phases. We address the issue of freezing and melting of spherical inclusions with a thermodynamically consistent model for nucleation of the new phase. The role of the matrix is included in the model through the contact angle of the liquid-solid interface on the matrix material, which strongly affects the nucleation behavior. We emphasize how the matrix curvature modifies the classical result for heterogeneous nucleation on a plane surface. The proposed formulation is simple and universal and can be easily used to analyze measurements. We illustrate the procedure on two recent experiments.

DOI: 10.1103/PhysRevB.77.184108 PACS number(s): 64.60.qe, 82.60.Nh, 64.70.D−, 82.60.Qr

I. INTRODUCTION

Nanotechnologies raise fundamental questions about the way macroscopic physical laws are modified at the nanoscale. For instance, our description of phase transitions has to be modified to describe nano-objects: since the pioneering experiments by Takagi,[1] it is known that the melting temperature of a crystal is size dependent. Nanocrystals (NCs) often melt at temperatures lower than the bulk melting point T_0, and the smaller the size, the larger the melting point shift.[2] This holds for most freestanding or supported NCs, which are in contact with their vapor. However, when NCs are embedded in another material, the melting point can be elevated. In addition, for all systems, hysteresis can be observed, illustrating the phenomenon of metastability:[3,4] melted NCs can be cooled down to temperatures at which the solid is the most stable phase, but nucleation of the solid is hindered by the energy cost of creating a liquid-solid interface. On the other hand, freestanding or supported NCs cannot be usually superheated because, in general, the liquid phase completely wets the solid, and melting starts from the outer surface. In embedded NCs, this mechanism can be suppressed if wetting is only partial, opening the way to the study of superheating. Melting will occur by heterogeneous nucleation at the NC/matrix wall.

Unfortunately, analysis of the size dependence of the melting point often ignores the nucleation process or at least neglects it for simplicity. The experimental melting temperature is rather compared to the theoretical values at which the solid becomes metastable or unstable (see, for instance, Refs. 5–12), although the actual nucleation temperature strictly lies in between these bounds.

The rate of heterogeneous nucleation on a plane surface was calculated with classical nucleation theory (CNT).[13] In the present paper, we show that, in NCs, the interface curvature strongly affects the usual result. A key parameter is the contact angle of the liquid-solid interface on the matrix, which results from the balance of interfacial tensions. Dealing with arbitrary contact angles and using nondimensional quantities allows us to give a universal formulation, which is easily applicable to any particular system. We hope that this will provide a useful tool for the analysis of future experiments. We begin with a summary of previous studies on melting of NCs (Sec. II). Then, we introduce the model (Sec. III) and compare it to experiments (Sec. IV). Finally, in Sec. V, we discuss the underlying approximations.

II. PREVIOUS STUDIES

Experimentally, free or supported NCs are often seen to melt below T_0.[2] Takagi[1] investigated the effect in layers of metal NCs, taking for the NC radii the thicknesses of the layers. Since then, numerous studies have more systematically measured the size dependence of the melting temperature.

Several models have been proposed to account for the melting point depression. They rely on different assumptions that are not always well understood. A clear review giving the historical references can be found in Ref. 14. Pavlov[15] proposed that melting occurs at the triple point equilibrium of the small particle, that is, the equilibrium between solid and liquid spheres of equal mass in contact with the vapor. His formula [Eq. (4) of Ref. 15] involving saturation and sublimation pressures can be rewritten to give the melting point T_m^{TP} of a solid sphere of radius R [Eq. (44) of Ref. 16],

$$\Delta T_m^{TP} = T_m^{TP} - T_0 = -\frac{2T_0}{LR}\left[\gamma_{SV} - \gamma_{LV}\left(\frac{\rho_S}{\rho_L}\right)^{2/3}\right], \qquad (1)$$

where L is the latent heat *per unit volume of the solid*, ρ_i is the density of phase i, and γ_{ij} is the surface tension between phases i and j, where i and j take the values L for liquid, S for solid, and V for vapor, respectively.

However, Pavlov's triple point analysis is relevant to the case of a set of liquid and solid spheres of equal mass, with no net mass exchange through the vapor.[17] In an experiment,

one may rather observe the melting of one isolated crystal. If the liquid completely wets the solid, a spherical shell will grow at the crystal surface, and the solid will not be in contact with the vapor. Rie[18] considered a solid sphere in equilibrium with a surrounding bulk liquid phase and obtained

$$\Delta T_m^{Rie} = T_m^{Rie} - T_0 = -\frac{2T_0}{LR}\gamma_{LS}. \quad (2)$$

Reiss and Wilson[17] explained that the melting of one solid sphere would occur at its equilibrium temperature with a liquid sphere of the same radius so that

$$\Delta T_m^{RW} = T_m^{RW} - T_0 = -\frac{2T_0}{LR}\left(\gamma_{SV} - \gamma_{LV}\frac{\rho_S}{\rho_L}\right). \quad (3)$$

If $\gamma_{LS}+\gamma_{LV}=\gamma_{SV}$,[17] and if we neglect the density change upon melting ($\rho_L=\rho_S$), Eqs. (1)–(3) are identical.

However, it was later realized that the above temperatures correspond to an *unstable* equilibrium.[19,20] For a given sphere, an energy barrier exists between the fully solid and the fully liquid phases. This barrier vanishes at T_0', which appears as an absolute limit of stability above which the solid cannot exist.[19,20] If $\gamma_{LS}+\gamma_{LV}=\gamma_{SV}$ and $\rho_L=\rho_S$, T_0' is given by Eq. (2).[19,20] On the other hand, no such stability limit is found for the liquid: freezing will occur through homogeneous nucleation,[3,4] explaining the large supercooling that can be obtained with molten NCs. Another interesting quantity arises: the temperature T_0'' at which the Gibbs' free energies of a frozen and a melted NC are equal,[20]

$$\Delta T_0'' = T_0'' - T_0 = -\frac{3T_0}{LR}(\gamma_{SV} - \gamma_{LV}), \quad (4)$$

where $\rho_L=\rho_S$ has been assumed. In this picture, at T_0'', the system can jump between both phases with an equal rate in both directions.[20] Melting will therefore occur by nucleation at a temperature T_m such that $T_0'' \leqslant T_m \leqslant T_0'$. Although a calculation of T_m is possible,[19] it appears to have been overlooked in many analysis of experiments: instead, one of the boundaries, T_0'' or T_0', is often used to fit the data on melting temperature as a function of radius.

In the case of NCs embedded in a matrix, an analogous T_0'' can be defined by replacing the vapor (V) by the matrix (M) in Eq. (4). The liquid does not necessarily wet the solid completely, especially for embedded NCs. If $\gamma_{LS}+\gamma_{LM}>\gamma_{SM}$ and $\gamma_{LS}+\gamma_{SM}>\gamma_{LM}$, there is a contact angle of the liquid on the matrix $\theta_c=\arccos[(\gamma_{SM}-\gamma_{LM})/\gamma_{LS}]$ so that $\Delta T_0''$ can be rewritten as

$$\Delta T_0'' = T_0'' - T_0 = -\frac{3T_0}{LR}\gamma_{LS}\cos\theta_c \quad (5)$$

As we shall see, within this model, there is no absolute limit at which the solid becomes unstable: melting will occur by nucleation above T_0''.

The limiting case $R\to+\infty$ corresponds to heterogeneous nucleation on a plane surface.[13] However, the theory needs to be modified when the size of the critical nucleus becomes non-negligible compared to R. Cantor and Doherty[21] seem to be the first to have considered the effect of the substrate curvature, but they included only a first order correction, which fails at small R. A partial wetting model was proposed by Cleveland *et al.*[22] for freestanding NCs. They considered the microcanonical ensemble and a geometry of two interpenetrating spheres but did not allow the LS interface to adopt a curvature different from the SV one. More recently, Xu *et al.*[23] proposed a nucleation model for embedded NCs to interpret their experimental finding of a large hysteresis of melting and freezing of Ge in amorphous silica (a-SiO_2). Because the hysteresis is symmetric around T_0, they deduced from Eq. (5) that $\theta_c=\pi/2$ and $\gamma_{LM}\simeq\gamma_{SM}$ and performed the calculation of the nucleation temperatures for this particular case. $\theta_c=\pi/2$ is a coincidence due to the specific properties of the system studied. It may vary for other materials, and we shall discuss an example later. This is what motivates our generalization of the theory of Xu *et al.* to the case of an arbitrary θ_c.

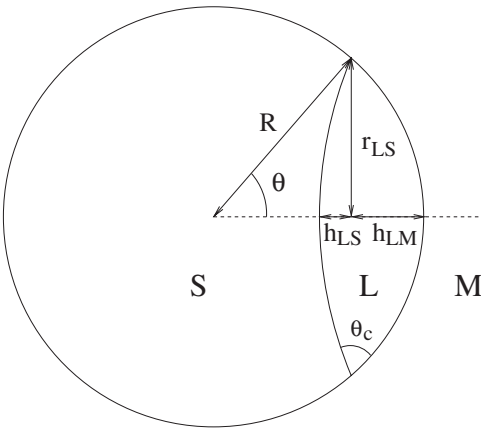

FIG. 1. Sketch of a liquid nucleus (L) in the metastable solid phase (S) for a cluster embedded in a matrix (M).

III. NUCLEATION IN THE CASE OF AN ARBITRARY WETTING ANGLE

We use CNT to calculate the energy barrier for heterogeneous nucleation in a spherical inclusion of radius R at a temperature $T=T_0+\Delta T$, with an arbitrary contact angle θ_c. We first consider melting at $T>T_0''$. The liquid phase will appear as a lenticular nuclei of volume V_L (Fig. 1). The contact angle of the liquid on the matrix being fixed at θ_c, the nuclei is fully characterized by the azimuthal angle θ of its circular boundary. Let S_{LS} and S_{LM} be the areas of the interfaces between the two phases and between the liquid and the matrix, respectively; the other notations are given in Fig. 1. Trigonometry gives the following relations:

$$r_{LS}(\theta) = R\sin\theta, \quad (6)$$

$$h_{LM}(\theta) = R(1-\cos\theta), \quad (7)$$

$$h_{LS}(\theta) = R[1-\cos(\theta_c-\theta)]\frac{\sin\theta}{\sin(\theta_c-\theta)}, \quad (8)$$

$$V_L(\theta) = \frac{\pi}{6} h_{\mathrm{LM}}(\theta)\,[3r_{\mathrm{LS}}(\theta)^2 + h_{\mathrm{LM}}(\theta)^2] + \frac{\pi}{6} h_{\mathrm{LS}}(\theta)\,[3r_{\mathrm{LS}}(\theta)^2 + h_{\mathrm{LS}}(\theta)^2], \tag{9}$$

$$S_{\mathrm{LS}}(\theta) = \pi\,[r_{\mathrm{LS}}(\theta)^2 + h_{\mathrm{LS}}(\theta)^2], \tag{10}$$

$$S_{\mathrm{LM}}(\theta) = \pi\,[r_{\mathrm{LS}}(\theta)^2 + h_{\mathrm{LM}}(\theta)^2]. \tag{11}$$

In the following, we neglect the density difference between liquid and solid ($\rho_S = \rho_L = \rho$), and we consider that the inclusion remains a sphere of radius R throughout the nucleation process. We also take the external pressure to be constant at P_0. One has then to consider the Gibbs free energy change, which writes

$$\Delta G(\theta) = G(\theta) - G(\theta = 0) = [\mu_L(T,P_0) - \mu_S(T,P_0)]\,\rho V_L(\theta) + \gamma_{\mathrm{LS}}\, S_{\mathrm{LS}}(\theta) + (\gamma_{\mathrm{LM}} - \gamma_{\mathrm{SM}})\, S_{\mathrm{LM}}(\theta), \tag{12}$$

where the difference in chemical potential between the two phases is taken *at a pressure equal to the external pressure*.[20] Finally, linearizing this difference gives

$$\Delta G(\theta) = -L\frac{\Delta T}{T_0} V_{\mathrm{L}}(\theta) + \gamma_{\mathrm{LS}}\, S_{\mathrm{LS}}(\theta) + (\gamma_{\mathrm{LM}} - \gamma_{\mathrm{SM}})\, S_{\mathrm{LM}}(\theta). \tag{13}$$

For each value of the pair $(\theta_c, \Delta T)$, $\Delta G(\theta)$ exhibits a maximum, which corresponds to the energy barrier for nucleation of the liquid in the solid, $E_b^{S\to L}(\theta_c, \Delta T)$. The case of freezing at $T < T_0''$ can be treated by a simple symmetry: $E_b^{L\to S}(\theta_c, \Delta T) = E_b^{S\to L}(\pi - \theta_c, -\Delta T)$. There is a correspondence between the melting of a superheated NC and the freezing of a supercooled nanodroplet. This holds only inasmuch the density difference between liquid and solid has been neglected. In the following, we will simply write E_b for the energy barrier, the direction of the phase change being implicitly given by the comparison between T and T_0''.

It is useful to introduce the following quantities:

$$\Delta T_{\max} = \frac{3T_0\gamma_{\mathrm{LS}}}{L\mathrm{R}}, \tag{14}$$

$$E_1 = \pi R^2 \gamma_{\mathrm{LS}}, \tag{15}$$

$$E_2 = E_b(\theta_c, \Delta T_0''), \tag{16}$$

$$E_3 = \frac{\pi}{3}(2 + \cos\theta_c)(1 - \cos\theta_c)^2 \gamma_{\mathrm{LS}} R_c^2, \tag{17}$$

$$R_c = \frac{2\gamma_{\mathrm{LS}}}{L}\frac{T_0}{|\Delta T|}. \tag{18}$$

$\Delta T_{\max}$ is the maximum melting point shift that can be obtained for a given inclusion: $\Delta T_0'' = -\Delta T_{\max}$ for $\theta_c = 0$ and $\Delta T_0'' = \Delta T_{\max}$ for $\theta_c = \pi$ [see Eq. (5)]. E_1 is an appropriate energy scale for the problem: it is the surface energy of a disk of radius R between L and S. E_2 is the energy barrier separating L and S phases at T_0'' (see below). E_3 is the energy barrier for heterogeneous nucleation on a plane surface.[13] R_c is the critical radius for homogeneous nucleation.[4] These definitions allow us to form several reduced quantities,

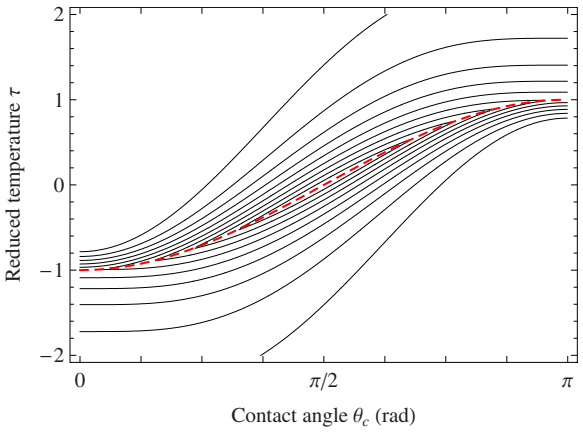

FIG. 2. (Color online) Contour plot of the reduced energy barrier ϵ_1 in the θ_c-τ plane. The solid curves show the contours from $\epsilon_1 = 0.9$ (innermost contour) to $\epsilon_1 = 0.1$ (outermost contour), every 0.1. Melting and freezing occur above and below the dashed red line, respectively.

$$\tau = \frac{\Delta T}{\Delta T_{\max}}, \tag{19}$$

$$\epsilon_i = \frac{E_b}{E_i} \quad \text{with } i \in \{1,2,3\}. \tag{20}$$

The ϵ_i thus defined are functions of τ, θ_c, and θ only. E_b is reached for

$$\theta_b = \arccos\left(\frac{3\tau + 2\cos\theta_c}{\sqrt{4 + 9\tau^2 + 12\tau\cos\theta_c}}\right). \tag{21}$$

The expression of E_b itself is complicated and will not be displayed here, but it is easily obtained from Eq. (13).

We now give a series of figures to illustrate the model. Figure 2 shows a contour plot of the reduced energy barrier for heterogeneous nucleation, ϵ_1, in the θ_c-τ plane. As the scaling energy E_1 is the same for each point of this plane, this allows a direct comparison of the barrier heights. The barrier vanishes only on two particular lines: $(\theta_c = 0, \tau \geqslant -2/3)$, corresponding to the limit of stability of a solid completely wet by its liquid (see Sec. II), and $(\theta_c = \pi, \tau \leqslant 2/3)$, corresponding to the symmetric case of the limit of stability of a liquid completely wet by its solid. For θ_c strictly between 0 and π, in the present model, E_b never reaches 0: there is no limit of stability; yet, nucleation will occur when E_b becomes small enough (see Sec. IV).

Figure 3 shows the maximum value of ϵ_1 for each θ_c, reached at T_0'', that is along the line $\tau = -\cos\theta_c$ (dashed red line in Fig. 2). The barrier is highest for $\theta_c = \pi/2$, where it reaches E_1, and lowest at $\theta_c = 0$ or π, where it reaches $16E_1/27$, reproducing the previous result for $\theta_c = 0$.[19,20]

To emphasize the variation of E_b with τ at a fixed θ_c, Fig. 4 shows a contour plot of the reduced barrier ϵ_2 in the θ_c-τ

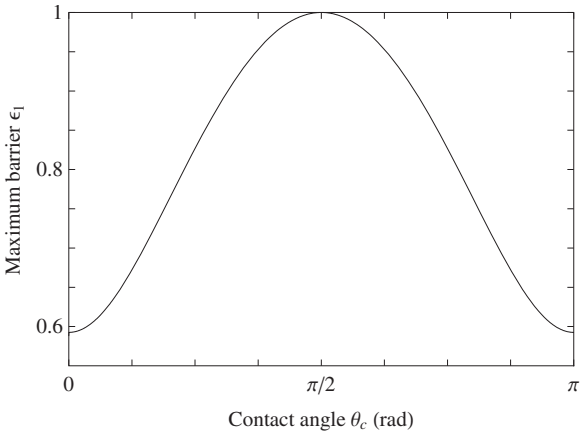

FIG. 3. Maximum of the reduced energy barrier ϵ_1 as a function of the contact angle θ_c.

plane. As expected, if $\theta_c < \pi/2$, $E_b(\tau)$ is steeper for the superheated crystal than for the supercooled liquid, and the situation is reversed for $\theta_c > \pi/2$.

It is also interesting to compare the present result to the classical one for heterogeneous nucleation on a plane surface, for which the energy barrier is E_3 [Eq. (17)].[13] We also introduce R_c, which is the critical radius for homogeneous nucleation [Eq. (18)].[4] At a given temperature $T \geqslant \max(T_0, T_0'')$, we can define $\eta = R/R_c = 3\tau/2$ and $\epsilon_3 = E_b/E_3$. The case of freezing at $T \leqslant \min(T_0, T_0'')$ is obtained with the above mentioned symmetry and with $\eta = R/R_c = -3\tau/2$. Figure 5 shows a contour plot of ϵ_3 for melting in the θ-η plane. This graph shows that for any given temperature above T_0, the classical result for heterogeneous nucleation on a plane surface is recovered for $R \gg R_c$, as expected. Note that although ϵ_3 vanishes at T_0, E_b does not: this behavior arises from the divergence of R_c and E_3 at T_0. Note also that for $\theta_c \to 0$, ϵ_3 is only defined by taking the limit, being the ratio of two vanishing quantities. One may use Fig. 5 to see below which size of the inclusion it becomes necessary to use the present model instead of the classical model for heterogeneous nucleation on a plane surface. The effect of confinement on melting or on freezing should be more easily seen in a system with a low or high value of θ_c, respectively.

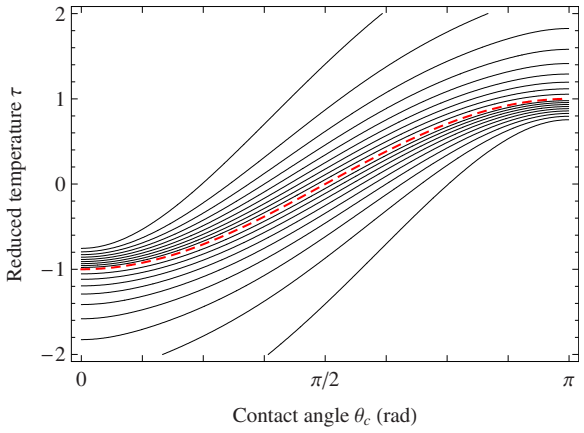

FIG. 4. (Color online) Contour plot of the reduced energy barrier ϵ_2 in the θ_c-τ plane. The solid curves show the contours from $\epsilon_2 = 0.9$ (innermost contour) to $\epsilon_2 = 0.1$ (outermost contour), every 0.1. Melting and freezing occur above and below the dashed red line (where $\epsilon_2 = 1$), respectively.

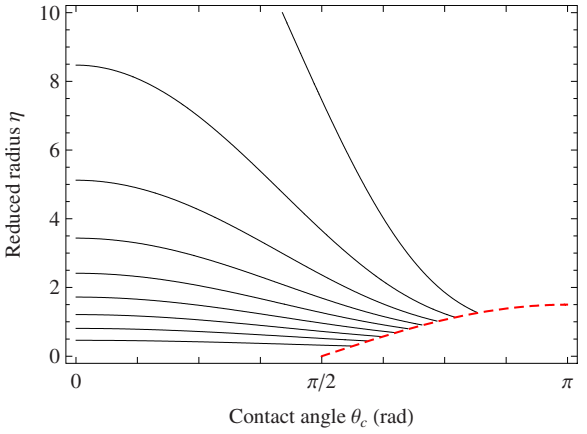

FIG. 5. (Color online) Contour plot of the reduced energy barrier ϵ_3 for melting in the θ_c-η plane. The solid curves show the contours from $\epsilon_3 = 0.1$ (bottom) to $\epsilon_3 = 0.9$ (top), every 0.1. ϵ_3 is not defined in the bottom right corner under the dashed red line.

IV. COMPARISON WITH EXPERIMENTS

There are numerous studies of NCs embedded in a matrix. Some of them exhibit melting of the NCs at a temperature higher than the bulk. Most of these involve NCs in a *crystalline* matrix: the high melting temperature is attributed to the existence of a coherent interface between the NC and the matrix, stabilizing the NC by epitaxy.[24] Because of the possible role played by epitaxy, the present model may not be relevant to address the case of a crystalline matrix. On the other hand, it is appropriate for the analysis of NCs embedded in an *amorphous* matrix, a system which has recently been prepared by ion implantation in a-SiO_2.

Once the energy barrier is calculated, the nucleation rate Γ is deduced from

$$\Gamma = N_s \nu \exp\left(-\frac{E_b}{k_B T}\right), \tag{22}$$

where $N_s = 4\pi R^2 \rho_S^{2/3}$ is the number of atoms in contact with the matrix and ν is an attempt frequency per atom, which is taken to be 10^{11} s^{-1}.[23] Assuming a nucleation rate of $\Gamma_{expt} = 1$ s^{-1} to be experimentally observable, one finds the nucleation temperatures for freezing and melting of NCs by solving

$$E_b = k_B (T_0 + \Delta T) \ln\left(\frac{N_s \nu}{\Gamma_{expt}}\right). \tag{23}$$

Note that other choices are possible for the prefactor of the exponential in Eq. (22).[3,4] Nevertheless, it affects only slightly the nucleation temperatures because of their logarithmic dependence on the prefactor.

An experiment measures the nucleation temperatures for melting T_m and for freezing T_f. From these two values and the known values of T_0, L, and R, we can deduce the two

unknowns of the present model, γ_{LS} and θ_c. We use the following procedure. T_m gives the corresponding energy barrier E_b^{expt} [Eq. (23)]. We start with an arbitrary value of γ_{LS}, which defines a corresponding scaling temperature ΔT_{max} [Eq. (14)] and energy E_1 [Eq. (15)]. Then, we adjust θ_c to give the correct $\epsilon_1 = E_b^{expt}/E_1$ at $\tau_m = (T_m - T_0)/\Delta T_{max}$. The pair (γ_{LS}, θ_c) can now be used to predict T_f. Finally, γ_{LS} is varied until the predicted T_f equals the experimental one. To the retained γ_{LS} now corresponds a value of θ_c that reproduces at the same time the experimental T_m and T_f. Now, the model is able to predict, without any additional parameter, T_m and T_f for inclusions with other radii.

Xu *et al.*[23] studied Ge in a-SiO_2 by electron diffraction. They observed a large melting point hysteresis nearly symmetric around T_0. From the symmetry, they propose that $\gamma_{LM} \simeq \gamma_{SM}$, and they develop a particular case of the present nucleation model ($\theta_c = \pi/2$). In their experiment, the melting and freezing transitions are around 100 K wide; this broadening is mainly due to the polydispersity of NCs (average $R = 2.5$ nm, rms deviation of 1.3 nm). Taking the midpoints gives $T_m \simeq 1400$ K and $T_f \simeq 930$ K. With $\theta_c = \pi/2$, they found that $\gamma_{LS} = 260$ mJ m^{-2} best reproduces their results.[23] However, they used an outdated value for L. This was later corrected, leading to $\gamma_{LS} = 285$ mJ m^{-2}.[25] The predicted values of T_m and T_f are then 1411 and 955 K, respectively. For Ge, $T_0 = 1211.4$ K, $ML/\rho_S = 36.94$ kJ mol^{-1}, $\rho_S = 5323$ kg m^{-3}, and $M = 72.61$ g mol^{-1}.[26] If we simultaneously solve for γ_{LS} and θ_c, following the above described procedure, we can exactly reproduce the experimental T_m and T_f with $\gamma_{LS} = 288$ mJ m^{-2} and $\theta_c = 86.6°$. However, given the width of the transitions and the experimental uncertainty on temperature measurements (± 15 K),[23] the accuracy is not sufficient to distinguish θ_c from $\pi/2$. To illustrate the minute dependence of the results on the choice of the prefactor in Eq. (22), we have tried a different value of ν: using a typical optical phonon frequency $\nu = 10^{13}$ s^{-1} (2 orders of magnitude larger than the initial choice) leads to $\gamma_{LS} = 303$ mJ m^{-2} and $\theta_c = 86.9°$, that is, a change of 5% and 0.3%, respectively.

We have looked for other experimental results on which to test the present model. Recently, Tagliente *et al.*[27] studied indium (In) NCs in a-SiO_2 and found a thermal hysteresis loop. Again, because of polydispersity, the transitions are around 25 K wide. Taking the midpoints give $T_m \simeq 433$ K and $T_f \simeq 315$ K. A detailed analysis of their x-ray data allowed them to give the dependence of the melting temperature on the NC size (see Fig. 6). They fit their data with a modified version of Eq. (4),

$$T_m(R) = \left(1 + \frac{\Delta E}{\rho_S L}\right) T_0 - \frac{3T_0}{RL}\left(\gamma_{SM} - \gamma_{LM}\frac{\rho_S}{\rho_L}\right), \qquad (24)$$

where ΔE is the change in strain energy density on melting.[7] First of all, let us recall that this is an oversimplification: the last term in Eq. (24) corresponds to T_0'', which is the lower limit for melting point depression, and not to the nucleation temperature. They obtain a best fit of $T_m(1/R)$ (Fig. 6) with $\Delta E\ T_0/(\rho_S L) = 40$ K and a slope $-(3T_0/L)[\gamma_{SM} - \gamma_{LM}(\rho_S/\rho_L)] = -150.5$ K nm. For In, $T_0 = 429.75$ K, $ML/\rho_S = 3.281$ kJ mol^{-1}, $\rho_S = 7310$ kg m^{-3}, and $M = 114.82$ g mol^{-1}.[26] In this picture, $\Delta E > 0$ is needed to explain the fact that the largest NCs can be superheated. In principle, ΔE could be estimated from the theory of elasticity and from the x-ray measurement of the lattice constant of the NC; unfortunately, only its relative temperature variation is analyzed,[27] casting doubt even on its sign. Moreover, if we take $\rho_L = \rho_S$, we find $\gamma_{SM} - \gamma_{LM} = 24.4$ mJ m^{-2}. This is a rather low value; if we compare to those obtained from undercooling experiments on droplets[28,29] ($\gamma_{LS} = 30.8$ or 30.6 mJ m^{-2}) or from liquid correlation lengths[30] ($\gamma_{LS} = 31 \pm 2$ mJ m^{-2}), we expect partial wetting of the matrix. The present model should then be preferably used. For the transition temperatures, we use the midpoints given above. As for the radius, we take the one that corresponds to $T_m \simeq 433$ K in Fig. 6: $R = 4$ nm. The above described procedure (with $\nu = 10^{11}$ s^{-1}) gives $\theta_c = 52°$ and $\gamma_{LS} = 31.6$ mJ m^{-2}, which is in excellent agreement with published values.[28–30] With these numbers, we can now compute T_m for other radii: the experimental data are well reproduced, without any additional parameter (see Fig. 6). As a further check, we have tried to describe the data with nucleation theory in the case of complete wetting ($\theta_c = 0$). The absolute values of T_m and T_f cannot be reproduced without introducing elastic effects [ΔE in Eq. (24)]. Yet, we have tried to fit $T_m - T_f$: to reproduce the experimental value for $R = 4$ nm requires $\gamma_{LS} = 35.5$ mJ m^{-2}, but then the average slope of $T_m(1/R)$ is 32% too large (−198 K nm). This excludes a simple explanation by a constant shift due to an elastic effect and confirms that our model with partial wetting reproduces the measurements better.

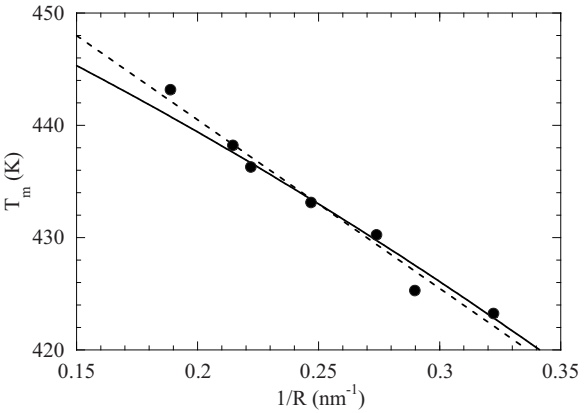

FIG. 6. Nucleation temperature for melting of In NCs in a-SiO_2 as a function of their inverse radius. The solid circles are experimental data (Ref. 27), the dashed line is a fit with Eq. (24), and the solid curve shows the prediction of the present model, with $\gamma_{LS} = 31.6$ mJ m^{-2} and $\theta_c = 52°$.

V. DISCUSSION

The two examples discussed above show that the present model is able to give a satisfactory account of the data. It makes, however, some approximations that are worth discussing.

Macroscopic thermodynamics has been used to describe microscopic systems. In particular, the volume and surface contributions to the energy have been separated, although the

interface between the two phases may not have a negligible thickness compared to that of the phases that are assumed homogeneous. Similar criticisms have often been discussed in the context of nucleation theory.[3,4]

In a similar way, the present treatment neglects the interaction between interfaces. In the case of complete wetting of the solid-vapor interface by the liquid, some models have included this interaction. They write the surface energy change per unit area when creating a liquid layer of thickness z as $(\gamma_{LS}+\gamma_{LV}-\gamma_{SV})[1-\exp(-z/\xi)]$, where ξ is the microscopic interaction range. This ensures continuity between the state with and without liquid. This theory has been developed in the context of surface melting.[31] The flat surface of a bulk solid is seen to melt over a few atomic layers at temperatures below melting, and the liquid thickness diverges at T_0. In this frame, melting of NCs starts from the outside, leading to coexistence between a solid core and a liquid shell in some temperature range, before the NCs suddenly melts totally.[32] However, this theory requires an additional parameter, ξ, which is usually fitted to reproduce the data on NC melting. In addition, it is not clear how to extend this approach to the case of partial wetting.

An issue more specific to inclusions is the role of elasticity. It has been neglected here, but may be important, because of the volume change upon melting and because the embedded material and the matrix have different thermal expansion coefficients. In principle, elasticity can be included in the analysis,[7,25,33] but information is needed on the stress state of the system. It depends on materials, fabrication process, and thermal treatment.[34] In addition, in the case of an arbitrary contact angle, the spherical symmetry is lost, and the analysis becomes more involved.

Of course, these limitations could be overcome by performing microscopic simulations with appropriate interaction potentials.[2] However, such simulations require accurate information that is system specific. We believe that the present treatment within CNT provides a simple and universal tool to reproduce the main features of the experiments.

VI. CONCLUSION

We have proposed a model for freezing and melting of spherical inclusions in a host matrix. We have described a procedure that allows us to deduce the model parameters (surface tension γ_{LS} and contact angle θ_c of the liquid-solid interface) from the measured melting and freezing temperatures. Xu *et al.*[23] studied the particular case of Ge NCs in a-SiO_2, for which $\theta_c \simeq \pi/2$. We have already found another experiment[27] (on In NCs in a-SiO_2), which is well described by the model, including the observed dependence of the melting temperature on NC radius. The use of nondimensional quantities makes the use of this model for any particular system straightforward. We hope that it will provide a sound basis for the interpretation of future work on NCs in an amorphous matrix and that it will supersede the use of formulas that give only bounds on the nucleation temperature. Investigation of different materials and narrower distributions of NC radii, with different average values, would be of particular interest.

ACKNOWLEDGMENT

We thank Arezki Boudaoud for helpful discussions.

*caupin@lps.ens.fr

[1] M. Takagi, J. Phys. Soc. Jpn. **9**, 359 (1954).
[2] F. Baletto and R. Ferrando, Rev. Mod. Phys. **77**, 371 (2005).
[3] P. G. Debenedetti, *Metastable Liquids* (Princeton University Press, Princeton, NJ, 1996).
[4] S. Balibar and F. Caupin, C. R. Phys. **7**, 988 (2006).
[5] C. J. Coombes, J. Phys. F: Met. Phys. **2**, 441 (1972).
[6] Ph. Buffat and J.-P. Borel, Phys. Rev. A **13**, 2287 (1976).
[7] G. L. Allen, W. W. Gile, and W. A. Jesser, Acta Metall. **28**, 1695 (1980).
[8] G. L. Allen, R. A. Bayles, W. W. Gile, and W. A. Jesser, Thin Solid Films **144**, 297 (1986).
[9] A. N. Goldstein, C. M. Echer, and A. P. Alivisatos, Science **256**, 1425 (1992).
[10] K. M. Unruh, T. E. Huber, and C. A. Huber, Phys. Rev. B **48**, 9021 (1993).
[11] H. Itoigawa, T. Kamiyama, and Y. Nakamura, J. Non-Cryst. Solids **210**, 95 (1997).
[12] M. Zhang, M. Yu. Efremov, F. Schiettekatte, E. A. Olson, A. T. Kwan, S. L. Lai, T. Wisleder, J. E. Greene, and L. H. Allen, Phys. Rev. B **62**, 10548 (2000).
[13] D. Turnbull, J. Chem. Phys. **18**, 198 (1950); J. Appl. Phys. **21**, 1022 (1950).
[14] C. Faivre, D. Bellet, and G. Dolino, Eur. Phys. J. B **7**, 19 (1999).
[15] P. Pavlov, Z. Phys. Chem., Stoechiom. Verwandtschaftsl. **65**, 1 (1909); **65**, 545 (1909).
[16] K.-J. Hanszen, Z. Phys. **157**, 523 (1960).
[17] H. Reiss and I. B. Wilson, J. Colloid Sci. **3**, 551 (1948).
[18] E. Rie, Z. Phys. Chem., Stoechiom. Verwandtschaftsl. **104**, 354 (1923).
[19] P. R. Couchman and W. A. Jesser, Nature (London) **269**, 481 (1977).
[20] H. Reiss, P. Mirabel, and R. L. Whetten, J. Phys. Chem. **92**, 7241 (1988).
[21] B. Cantor and R. D. Doherty, Acta Metall. **27**, 33 (1979).
[22] C. L. Cleveland, U. Landman, and W. D. Luedtke, J. Phys. Chem. **98**, 6272 (1994).
[23] Q. Xu, I. D. Sharp, C. W. Yuan, D. O. Yi, C. Y. Liao, A. M. Glaeser, A. M. Minor, J. W. Beeman, M. C. Ridgway, P. Kluth, J. W. Ager III, D. C. Chrzan, and E. E. Haller, Phys. Rev. Lett. **97**, 155701 (2006).
[24] Q. Jiang, Z. Zhang, and J. C. Li, Chem. Phys. Lett. **322**, 549 (2000).
[25] F. Caupin, Phys. Rev. Lett. **99**, 079601 (2007).
[26] *Handbook of Chemistry and Physics*, 85th ed., edited by D. R. Lide (CRC, Boca Raton, FL, 2004).
[27] M. A. Tagliente, G. Mattei, L. Tapfer, M. Vittori Antisari, and P. Mazzoldi, Phys. Rev. B **70**, 075418 (2004); M. A. Tagliente, L.

Tapfer, M. Vittori Antisari, G. Mattei, and P. Mazzoldi, J. Non-Cryst. Solids **345-346**, 663 (2004).
[28] V. P. Skripov, in *Crystal Growth and Materials*, edited by E. Kaldis and H. J. Scheel (North-Holland, Amsterdam, 1977), p. 328.
[29] J. H. Perepezko, Mater. Sci. Eng. **65**, 125 (1984). A maximum supercooling of 110 K is reported, from which we deduce γ_{LS}, with homogeneous nucleation theory.
[30] A. M. Molenbroek, G. ter Horst, and J. W. M. Frenken, Surf. Sci. **365**, 103 (1996).
[31] J. G. Dash, H. Fu, and J. S. Wettlaufer, Rep. Prog. Phys. **58**, 115 (1995).
[32] R. R. Vanfleet and J. M. Mochel, Surf. Sci. **341**, 40 (1995).
[33] J. J. Hoyt, Phys. Rev. Lett. **96**, 045702 (2006).
[34] I. D. Sharp, D. O. Yi, Q. Xu, C. Y. Liao, J. W. Beeman, Z. Liliental-Weber, K. M. Yu, D. N. Zakharov, J. W. Ager III, D. C. Chrzan, and E. E. Haller, Appl. Phys. Lett. **86**, 063107 (2005).